

# JGR Space Physics



## RESEARCH ARTICLE

10.1029/2020JA028923

## In Which Magnetotail Hemisphere is a Satellite? Problems Using in Situ Magnetic Field Data

A. De Spiegeleer<sup>1</sup> , M. Hamrin<sup>1</sup> , H. Gunell<sup>1</sup> , T. Pitkänen<sup>1,2</sup> , and S. Chong<sup>1</sup> 

<sup>1</sup>Department of Physics, Umeå University, Umeå, Sweden, <sup>2</sup>Space Physics and Astronomy Research Unit, University of Oulu, Oulu, Finland

### Key Points:

- Simulation and Cluster data show dents in the magnetic field lines ahead of high-speed flows
- Within a dent, Geocentric Solar Magnetospheric  $B_x > 0$  ( $B_x < 0$ ) is observed in the Southern (Northern) Hemisphere
- Thus, using the sign of the measured  $B_x$  to identify where a satellite is can lead to errors

### Supporting Information:

- Supporting Information S1
- Figure S1
- Movie S1

### Correspondence to:

M. Hamrin,  
[hamrin@space.umu.se](mailto:hamrin@space.umu.se)

### Citation:

De Spiegeleer, A., Hamrin, M., Gunell, H., Pitkänen, T., & Chong, S. (2021). In which magnetotail hemisphere is a satellite? Problems using in situ magnetic field data. *Journal of Geophysical Research: Space Physics*, 126, e2020JA028923. <https://doi.org/10.1029/2020JA028923>

Received 10 NOV 2020  
 Accepted 2 FEB 2021

**Abstract** In Earth's magnetotail plasma sheet, the sunward-tailward  $B_x$  component of the magnetic field is often used to separate the region above and below the cross-tail current sheet. Using a three-dimensional magneto-hydrodynamic simulation, we show that high-speed flows do not only affect the north-south magnetic field component (causing dipolarization fronts), but also the sunward-tailward component via the formation of a magnetic dent. This dent is such that, in the Northern Hemisphere, the magnetic field is tailward while in the Southern Hemisphere, it is earthward. This is opposite to the expected signatures where  $B_x > 0$  ( $B_x < 0$ ) above (below) the neutral sheet. Therefore, the direction of the magnetic field cannot always be used to identify in which hemisphere an in situ spacecraft is located. In addition, the cross-tail currents associated with the dent is different from the currents in a tail without a dent. From the simulation, we suggest that the observation of a dawnward current and a tailward magnetic tension force, possibly together with an increase in the plasma beta, may indicate the presence of a magnetic dent. To exemplify, we also present data of a high-speed flow observed by the Cluster mission, and we show that the changing sign of  $B_x$  is likely due to such a dent, and not to the spacecraft moving across the neutral sheet.

**Plain Language Summary** In the middle of the plasma sheet in the Earth's magnetotail exists an electrical current sheet that separates the magnetic field pointing away from (toward) Earth in the Southern (Northern) Hemisphere. This property of the magnetic field is usually used to identify the region of observation. However, by analyzing results from a three-dimensional simulation and in situ observations, we show that this property of the magnetic field may not always hold. Indeed, in the presence of a fast earthward flowing plasma confined near the current sheet region, the magnetic field may instead be observed to point toward (away from) Earth in the Southern (Northern) Hemisphere, that is, opposite to the usual configuration. This is because the fast earthward flow deforms the magnetic field lines in such a way that the field lines wrap around the forefront of the fast earthward flow. This wrapping of the magnetic field lines results in a magnetic field orientation opposite to what is expected, namely, it is earthward in the Southern Hemisphere and tailward in the Northern Hemisphere.

## 1. Introduction

Since the dawn of observational space physics, particle and magnetic field data have been used to distinguish between different plasma regions. For example, the textbook picture of the Earth's magnetotail plasma sheet is that the sunward-tailward  $B_x$  component of the magnetic field can be used to determine whether a spacecraft (earthward of the near-Earth neutral line) is located above or below the duskward cross-tail current sheet. In the Southern Hemisphere, which is below the current sheet, the magnetic field is normally directed tailward ( $B_x < 0$ ) while in the Northern Hemisphere, the magnetic field is earthward ( $B_x > 0$ ). Similarly, the sign of the dawn-dusk component,  $B_y$ , can in the simplified textbook picture give information in which local time sector (i.e., toward dusk or dawn) a spacecraft is located.

However, it is well-known that high-speed flows in the magnetotail (Baumjohann et al., 1989) deform the magnetic field lines, for example causing dipolarization fronts (DFs; e.g., Angelopoulos et al., 1992; Nakamura et al., 2002; Ohtani et al., 2004). DFs are seen as a sudden increase of the northward  $B_z$  magnetic field component at the front of the high-speed flows. While the northward component of the magnetic field associated with a dipolarization front (DF) has received significant attention, the earthward-tailward component has not been investigated much. In this article, we therefore investigate variations in the sign of  $B_x$

© 2021. The Authors.

This is an open access article under the terms of the [Creative Commons Attribution License](https://creativecommons.org/licenses/by/4.0/), which permits use, distribution and reproduction in any medium, provided the original work is properly cited.

since such variations are associated with dents in the magnetic field, which is another type of magnetic field deformation caused by high-speed flows. In a dent, the earthward flow deforms the magnetic field lines in such a way that the field lines wrap around the forefront of the flow. The magnetic field near the center of the plasma sheet is therefore pushed and bent toward the Earth, causing a magnetic field orientation opposite to what is expected from the standard textbook picture of a convex tail magnetic field configuration. The curvature vector of the magnetic field in the case of a dent is therefore earthward instead of tailward as for the standard case. Such dents can drastically affect the orientation of the magnetic field to the extent that ignoring them makes the usual identification of the spacecraft location by use of  $B_x$  and  $B_y$  incorrect.

The occurrence of magnetic field dents near high-speed reconnection flows have been predicted in early theoretical and modeling work. For example, using theoretical models of Petschek reconnection, Petschek and Thorne (1967) and Vasyliunas (1975) showed that magnetic dents can appear between the slow mode shocks, ahead of the reconnection exhausts. To our knowledge, such dent deformations were first observed in the magneto-hydrodynamic (MHD) simulations of Birn (1984) and Sato and Hayashi (1979), and they were suggested to be related to a reversal of the electrical cross-tail current. Even though dents have been observed in early theoretical and numerical investigations, they have not been discussed much in later years.

Birn et al. (2011) used a three-dimensional MHD simulation to study the breaking of a high-speed flow and its DF as it propagates toward the inner magnetosphere. It was found that the high-speed flow could rebound as it overshoots its equilibrium position (e.g., Chen & Wolf, 1999; Panov et al., 2010). In the figures presented in Birn et al. (2011), one can observe that, accompanying the DF ahead of the high-speed flow, there is a dent in the magnetic field lines. While observable in the figure, this feature was not discussed in the article by Birn et al. (2011). Instead, it was Nakamura et al. (2013) who noted the magnetic dent present in Birn et al. (2011). Nakamura et al. (2013) shortly mentioned that the dent associated a dawnward current density component (negative  $J_y$ ) related to the rebound of the high-speed flow when overshooting the equilibrium position near the inner magnetosphere. To the best of our knowledge, the study by Nakamura et al. (2013) is the only one which mentions dents in the magnetic field lines at the forefront of a high-speed flow.

Even though dents have not been discussed much in the literature, there is supporting evidence that dents at the front of high-speed flows exist. Karlsson et al. (2015) investigated the contributions of the magnetic pressure force and magnetic tension force within and in front of high-speed flows using Cluster data. While not mentioned in the article, one can observe that for some of the high-speed flows, a tailward tension force is observed. Such a tension force is expected for a magnetic dent.

In this study, we focus on investigating the features of magnetic dents which are related to earthward flows. Such an investigation is important because the sign of the earthward-tailward magnetic field component, which is commonly used to identify the magnetotail's hemispheres, changes in the presence of a magnetic dent and it can lead to the misidentification of the region in which a spacecraft is located.

With the intention of better understanding magnetic dents, we employ a three-dimensional MHD simulation in which we observe a dent in front of an earthward high-speed flow. We fly artificial spacecraft in the simulation in the neighborhood of the dent to investigate the signatures a real in situ satellite would measure in Earth's magnetotail. Observations obtained by these artificial spacecraft near the dent are compared to artificial spacecraft observations of the cross-tail current sheet in a standard textbook configuration, that is, in the absence of a magnetic dent. We highlight the risk of misidentifying the hemisphere in which a satellite is located. We also present data from the multi-spacecraft Cluster mission of a high-speed flow showing evidence of a magnetic dent.

## 2. Data

We use both a three-dimensional MHD simulation and in situ spacecraft observations for this study. In our analysis, we use the Geocentric Solar Magnetospheric system.

The simulation model used in this study is the three-dimensional MHD Block-Adaptive-Tree-Solarwind-Roe-Upwind-Scheme (BATS-R-US) model (Powell et al., 1999; Tóth et al., 2012) that is part of the Space

Weather Modeling Framework (Tóth et al., 2005). The simulation run was done at the Community Coordinated Modeling Center and has the run number Michael\_Hesse\_102416\_4. The simulation run is done using idealized conditions and has the following properties:

- $34.8 \times 10^9$  cells with a resolution of  $\frac{1}{16}R_E$  at the inner-boundary
- It uses the ionospheric model by Ridley et al. (2004)
- There is no dipole tilt
- The solar wind velocity, density, and temperatures are kept constant at  $V_{GSM} = (-400, 0, 0)$  km/s,  $5 \text{ cm}^{-3}$  and 232100 K, respectively
- The interplanetary magnetic field is  $B_z = -5$  nT at the start of the simulation run. After 1 h, the field is slowly rotated (in 30 min) to  $B_y = 5$  nT
- The simulation starts at an arbitrary time at 11:00:00 and is run for a total of 4.5 h

All plots of the simulation run will be shown on a rebinned grid with a  $1/8R_E$  cell-size which is the original resolution in the magnetotail region. Hence, the plots will have lower resolution near-Earth and higher resolution toward the flanks than they truly have in the simulation run. This is not a problem as we do not study those regions. All the plots are made using the plotting tools developed by De Spiegeleer (2020).

The in situ data are taken from the Cluster multi-spacecraft mission (e.g., Escoubet et al., 1997, and references therein). We use the Cluster Ion Spectrometry - COmposition and DIstribution Function analyser (CIS-CODIF) instrument for the proton  $H^+$  data which have a 4 s resolution (Rème et al., 2001) and the FluxGate Magnetometer instrument for the magnetic field data with a resolution of five vectors per second (Balogh et al., 2001).

### 3. Simulation Results

In this section, we present the simulation results. We investigate the signatures of a magnetic dent associated with a DF at a high-speed earthward flow off the equatorial plane.

#### 3.1. Overview

We present the state of the plasma sheet ( $z = 0$ ) at time 12:23:00 in Figure 1a. A DF can be observed as an increase of  $B_z$  (Figure 1a, color plot with colorbar to the right) near  $x = -17R_E$  for  $|y| < 5R_E$ . Just tailward of the DF are fast earthward flows with speed  $>400$  km/s (Figure 1a, quiver plot with the colorbar to the left indicating the speed) which will be referred to as high-speed flows.

We study the transverse ( $xz$  plane) signatures of the DF and its associated high-speed flow at  $y = -2.875R_E$  by showing the velocity along  $x$ ,  $V_x$  (Figure 1b, color plot) and some magnetic field lines uniformly separated in  $x$  at  $z = 0$  (Figure 1b, black lines). The change in color of the field lines depends on whether they are in front ( $y > -2.875R_E$ , darker) or behind ( $y < -2.875R_E$ , lighter) the cut at  $y = -2.875R_E$ .

From the enhanced  $B_z$  magnetic field in Figure 1a (light red; and in agreement with the field lines in Figure 1b), we see that the DF is located near  $x = -17R_E$ . Earthward of the DF, we observe the typical convex geometry of the tail magnetic field in the absence of a dent, but we can see a dent in the magnetic field lines just tailward of the DF region. This dent looks as if the magnetic field lines are wrapped around the head of the high-speed flow. In the dent region,  $B_x > 0$  in the Southern Hemisphere and  $B_x < 0$  in the Northern Hemisphere. This means that the sign of  $B_x$  is opposite to the usually expected sign for the hemisphere where the spacecraft is located, and this could cause problems when identifying the hemisphere using in situ  $B_x$  measurements only (see Section 4).

In Movie S1, we show a three-dimensional view of the dent from the simulation. The dent can clearly be seen in the  $xz$  plane.

In addition, we see that some field lines are deformed in the  $y$  direction. This affects the sign of  $B_y$  depending on where the observation is done (e.g., by an artificial spacecraft in the simulation) with respect to the dent. This has to be considered together with other effects involving  $B_y$  (e.g., Pitkänen et al., 2019) to determine in which local time sector a spacecraft is located. However, it should be noted that the deformation of  $B_y$  is

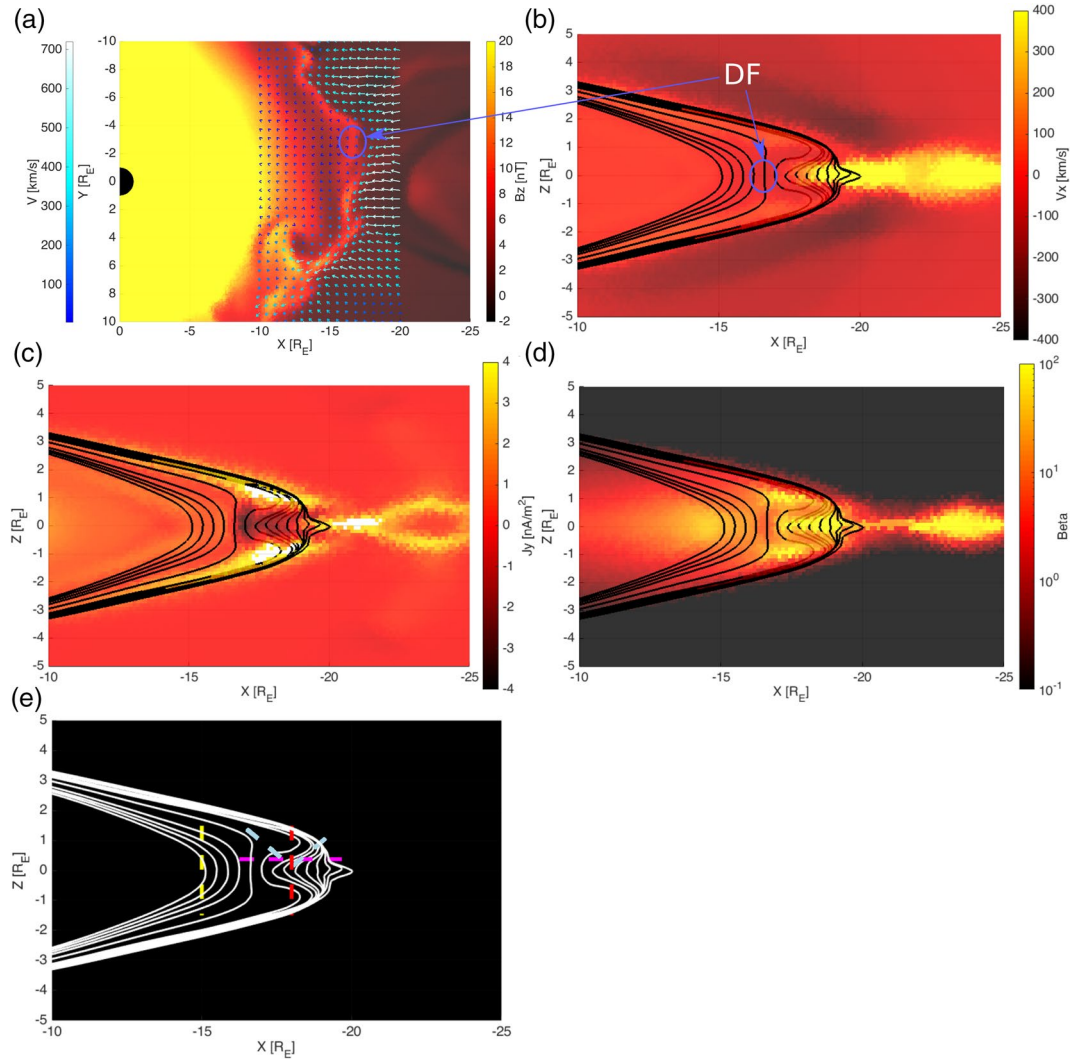


**Figure 1.** Three-dimensional MHD simulation snapshot of the magnetotail at time 12:23:00. (a) The plane at  $z = 0$ . The northward magnetic field  $B_z$  is shown using a color plot and the plasma velocity  $V$  using a quiver plot. The color of the arrows indicates the speed. (b) The plane at  $y = -2.875R_E$ . The color plot shows  $V_x$ , the plasma velocity along  $x$ . A few magnetic field lines are shown in black and gray. They are each separated by  $0.5R_E$  at  $z = 0$ , and the field lines are lighter if they are at  $y < -2.875R_E$ . The dipolarization front (DF) is indicated in panels a and b with arrows. (c) and (d) Same as (b) but showing the current density in the dawn-dusk direction ( $J_y$ ) and the plasma beta parameter ( $\beta$ ). (e) The field lines are now shown in white and the dashed lines show four artificial spacecraft crossings: vertical earthward of the dent (yellow), vertical in the dent (red), horizontal (magenta), and v-shaped (light blue). The data associated to these crossings are shown in Figures 2a–d.

complicated as indicated by the supporting information, and it is outside the scope of the present study to categorize the  $B_y$  deformation in detail.

Because of the dent-like geometry of the magnetic field lines, the electrical current system differs from the standard neutral sheet configuration. Now there is a dawnward current in the center of the plasma sheet and two regions of duskward currents; one above and one below (near  $|z| = 1R_E$ ) the center of the plasma sheet. In this configuration (Figure 1c), the dawnward current ( $J_y < 0$ ) located at the center of the plasma sheet can be caused either by the increase of  $B_z$  along  $x$  or by the decrease of  $B_x$  along  $z$  according to Ampère's law in a steady-state. In the dent, near the DF in the simulation,  $J_y < 0$  is mostly due to the DF because  $\partial B_z / \partial x = \partial_x B_z > 0$  while farther downtail, the dawnward current is caused by the  $\partial_z B_x < 0$  term. We hence note that  $J_y < 0$  is not only a property of the magnetic dent geometry but it can also occur due to a DF

(e.g., Yao et al., 2013). It is therefore important to analyze the sign of  $\partial_z B_x$  to properly identify a dent, since  $B_x$  should vary along the north-south direction if a dent is present. Also the magnetic tension force along  $x$  should be analyzed in the neighborhood of the dent, since it would be oppositely directed as compared to the tension force in the absence of a dent.

### 3.2. Artificial Spacecraft Crossings

To better visualize what a spacecraft could observe in the vicinity of a magnetic field dent, we present artificial spacecraft data of four different trajectories. The trajectories of the satellites are crossings at a fixed time (12:23:00) in the simulation but will be interpreted as if the spacecraft moved through space with time. In addition and as a reference, we begin by presenting data from the crossing of the cross-tail current sheet in a normal textbook-like configuration. For each crossing, we show in Figure 2 the plasma velocity in the first panel, the magnetic field in the second panel, the current density in the third panel. In addition, we show the plasma beta and the plasma mass density in panel four and five for completeness, but these are not the main focus of the analysis.

In Figure 2a, we show the data associated with the north-south yellow crossing shown in Figure 1e. This crossing is earthward of the dent, in a more textbook-like configuration of the tail magnetic field. The artificial satellite is initially located at  $(-15, -2.875, 1.5) R_E$  and it probes straight down to  $z = -1.5R_E$ . The signatures presented are thus due to the crossing of the cross-tail current sheet.  $B_x$  (2nd panel) is observed to change from positive to negative near  $z = 0$  which is the center of the plasma sheet as the spacecraft moves from the Northern to the Southern Hemisphere. A similar behavior is observed for  $B_y$  whereas  $B_z$  stays positive and nearly constant throughout. The duskward current density ( $J_y$  in the 3rd panel) is seen to decrease closer to the center of the plasma sheet and stays relatively constant between  $z \sim 1R_E$  and  $-1R_E$ . The plasma beta (4th panel) and the plasma mass density (5th panel) both reach a maximum when the satellite is close to  $0R_E$ .

Next, we consider the vertical crossing (red, Figure 1e) of the region with the magnetic dent (Figure 2b). The artificial satellite moves vertically down from  $z = 1.5$  to  $-1.5R_E$  at  $x = -17.875R_E$  and  $y = -2.875R_E$ . The high-speed flow is observed near  $z = 0$  and it is also where  $J_y < 0$  which is due to the dent in the magnetic field lines. Clearly, in the Northern Hemisphere and within the dent structure,  $B_x$  is negative while it is positive in the Southern Hemisphere. Because of this change of  $B_x$  along  $z$  in the dent,  $\partial_z B_x < 0$ . It is this variation of  $B_x$  that is the cause for the dawnward current ( $J_y < 0$ ). For this crossing, the artificial satellite measures duskward currents above and below the magnetic dent where  $B_x$  is also seen to change sign.

In Figure 2c, we show the data associated with the artificial satellite that moves solely along  $x$  (magenta crossing in Figure 1e). Here, the satellite traverses the dent in the Northern Hemisphere at  $z = 0.375R_E$  between  $x = -16.25$  and  $-20R_E$ . The change in the sign of  $B_x$  from positive to negative occurs near the DF around  $x = -16.5R_E$ . The value of  $B_z$  is seen to decrease from a maximum at about  $x = -17R_E$  as the spacecraft moves tailward. Associated with this decrease in  $B_z$  is the appearance of a dawnward current density ( $J_y < 0$ ). The current is dawnward because the artificial satellite probes behind the DF and thus  $\partial_x B_z > 0$  which causes  $J_y < 0$ . Tailward of  $x = -17.75R_E$  we see that  $B_z$  is fairly constant, and the dawnward current density is thus due to the  $\partial_z B_x < 0$  term which is a property of the magnetic dent.

Finally, we consider the v-shaped trajectory (light blue) in Figure 2d. Note that this trajectory can of course not correspond to a real trajectory due to the sharp angle, but it is used for practical reasons to display what type of signatures a spacecraft would observe if it moves in and out of the region of interest. For this v-shaped trajectory, the satellite is first in the Northern Hemisphere and starts above the magnetic dent, it then moves down and probes a bit of the main flow channel before moving above the dent again. We note that the satellite exits the plasma sheet at  $\sim x = -19R_E$ . When it is above the dent, the satellite observes a duskward current and a change in the sign of  $B_x$ . As it enters the dent, the satellite observes part of the fast flow and thus sees enhanced  $V_x$ . It is also at that point that the current density becomes clearly dawnward.

The above analysis of the artificial spacecraft crossings through the simulation has mainly focused on the signatures in the magnetic field and the cross-tail current in relation to the fast flow. Even though the mass density and the plasma beta have not been discussed in detail, one can note a difference between the case of

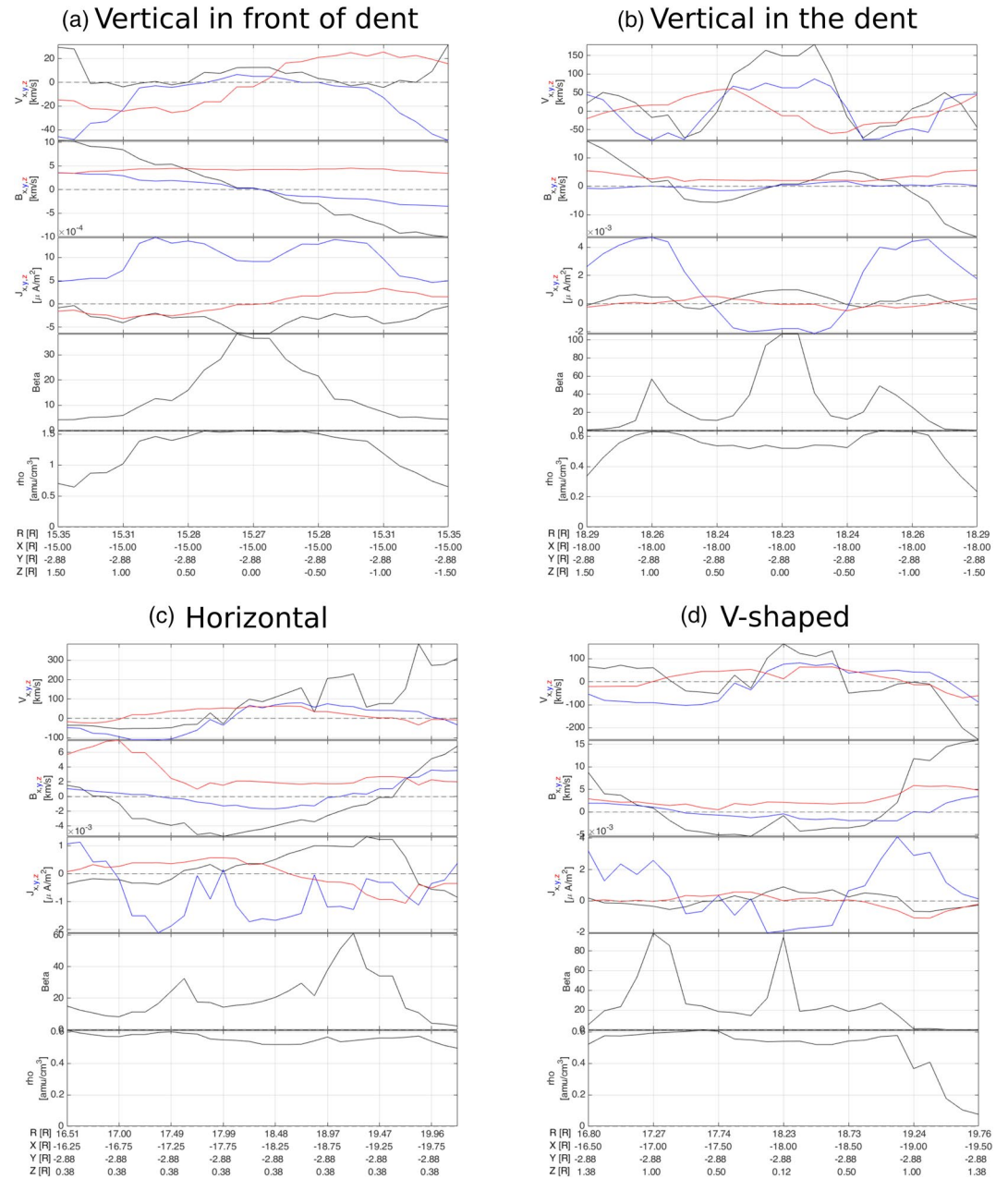


**Figure 2.** Artificial spacecraft crossings in the simulation in front of the dent (yellow, Figure 1e), vertically in the dent (red, Figure 1e), horizontally in the dent (magenta, Figures 1e) and a v-shaped crossing (light blue, Figure 1e). For each of the crossings, the layout of the data is the same. The first three panels of each subfigure (a)–(d) present the components of the velocity, the magnetic field and the current density, respectively. Panel four and five show the plasma beta and the mass density. (Note that the mass density is equivalent to the number density, since H<sup>+</sup> ions are considered).

a neutral sheet crossing in the more textbook-like magnetic field geometry outside the dent (Figure 2a) and the cases where the spacecraft probe the dent region (Figures 2b–d). In the normal magnetic field geometry, where the duskward cross-tail current is strong we see that there is a peak in the plasma beta and a (broader) peak in the mass density. However, in the dent geometry (Figures 2b–d) we see a more complicated trend with a tendency of a larger peak in the plasma beta in the neighborhood of a dawnward current (away from the center or the plasma sheet) than in the neighborhood of a duskward current. Investigating details in the (three-dimensional) variation of the plasma beta is, however, outside the scope of the present study.

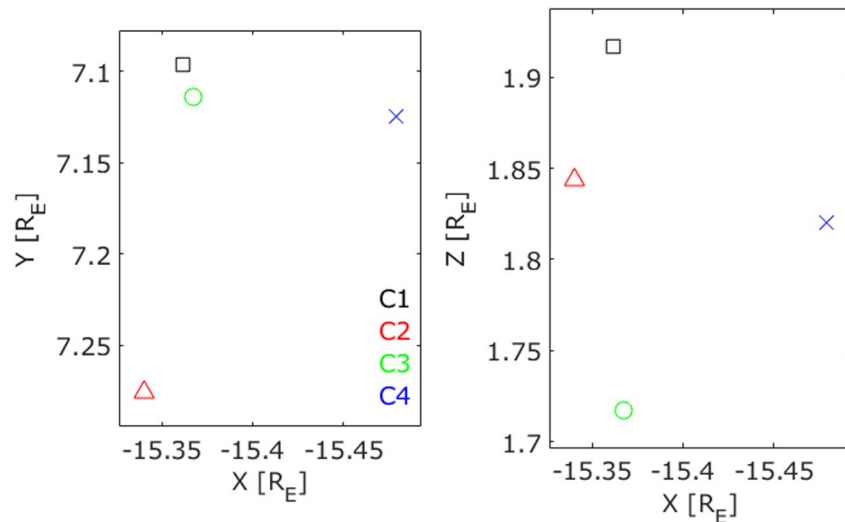


**Figure 3.** Position of the four Cluster satellites in the  $xy$  and  $xz$  planes.

#### 4. Cluster Observations

In this section, we analyze data from October 6, 2004, around 05:04 UTC when all four Cluster satellites observe a fast plasma flow near  $(-15.4, 7.2, 1.8) R_E$ . We show the position of the four Cluster satellites in Figure 3, and observed data ( $H^+$  energy-time spectrogram, plasma velocity, magnetic field, as well as the current density and the tension force and their components) in Figure 4.

Cluster 1 (C1), Cluster 3 (C3), and Cluster 4 (C4) probe approximately the  $xz$  plane in a nearly equilateral triangle (Figure 3), while Cluster 2 (C2) is significantly displaced along the  $y$  direction toward the dusk side. The elongation and the planarity of the tetrahedron spanned by the four spacecraft are 0.11 and 0.34, respectively, and the typical length scale is 1,001 km ( $\sim 0.16R_E$ ). The tetrahedral configuration allows us to use the methods presented in Paschmann and Daly (1998), for example, the curlometer method, to calculate the spatial derivatives of the magnetic field as well as the current density.

An overview of the high-speed flow data measured by Cluster 1 is shown in Figures 4a–c. The plasma velocity along  $x$ ,  $V_x$  (Figure 4b), reaches a maximum of 557 km/s at  $\sim 05:04:10$  UTC. At the beginning and end of the presented time interval,  $B_x > 0$  (Figure 4c) and this indicates that the satellite is located above the cross-tail current sheet before and after the fast flow. In the magnetic field data, a DF is observed at about 05:03:30 UTC. Also,  $B_x$  is observed to change sign from positive to negative during the high-speed flow, and then it turns back positive just before the end of the fast flow. In the following, we will show that this change to  $B_x < 0$  during the flow should not be misinterpreted as the spacecraft moving into the Southern Hemisphere for a short period of time. Instead, we will show that the sign change of  $B_x$  is likely caused by a dent in the magnetic field.

We show  $B_x$  measured by each of the four satellites in Figure 4d. The spacecraft observe the variations in the field at different times. Thus, we perform a timing analysis based on the decrease of  $B_x$  observed at around 05:30:35 UTC using the four satellites. The obtained time shifts are 4.79 s for C2,  $-0.41$  s for C3 and  $-1.30$  s for C4 with respect to the C1 observations. The time-shifted  $B_x$  data are shown in Figure 4e. It shows that the measured  $B_x$  is fairly similar between the satellites except for the time interval around 05:03:50 to 05:04:00 UTC (Figure 4e) when the measurements made by C2 differ significantly from the other satellites, possibly due to spatial and/or temporal variations. As discussed in Section 3.1, such deviations of the magnetic field away from the  $xz$  can be expected, but this implies that the curlometer technique may not be reliable using data from all four spacecraft. Because C2 measurements differ significantly from the other three spacecraft, we study the high-speed flow and the magnetic field signatures in two dimensions only (in the  $xz$  plane), ignoring the variations along  $y$  ( $\frac{\partial}{\partial y} = \partial_y = 0$ ). Therefore we do not use the full four spacecraft curlometer method for computing the current density and the tension force, but instead we use a three spacecraft

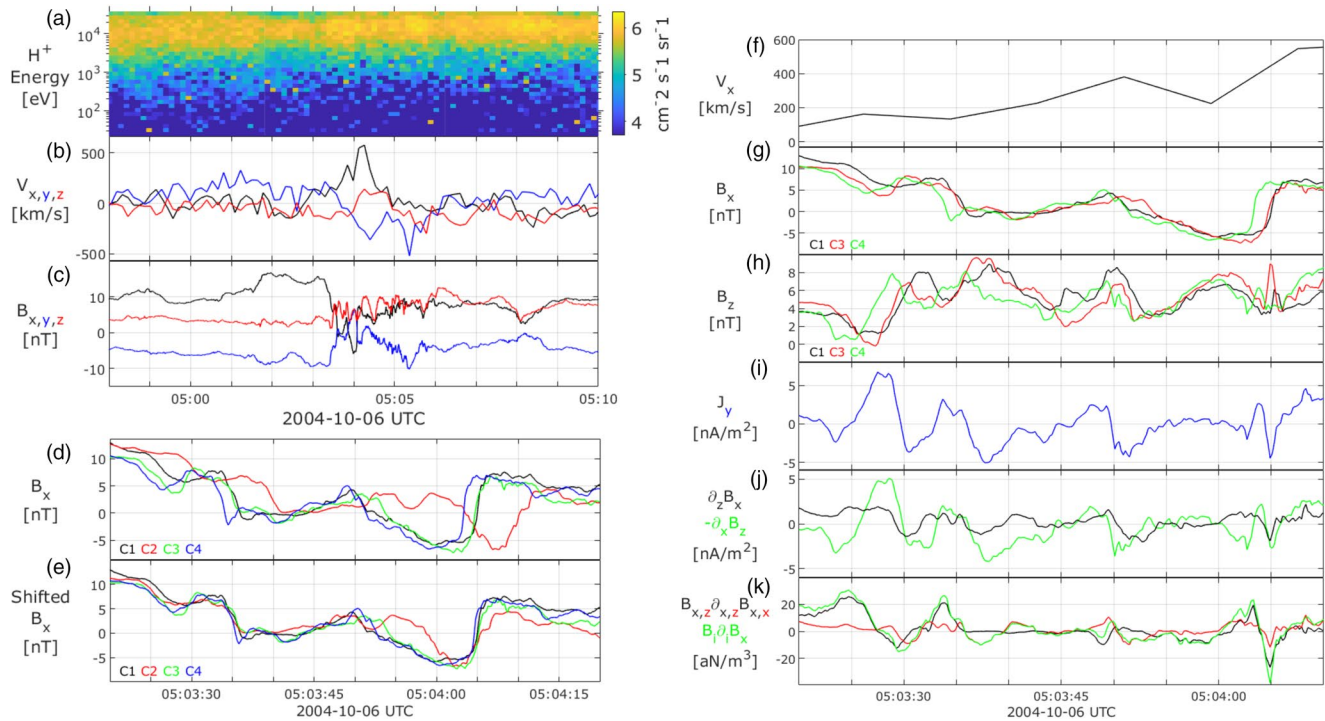


**Figure 4.** (a) Cluster 1 CIS-CODIF measurements of  $H^+$  differential energy flux. (b)  $H^+$  velocity moment from CIS-CODIF onboard C1. (c) Cluster 1 magnetic field data. (d) Magnetic field along  $x$  for all four Cluster satellites. (e)  $B_x$  data that have been time-shifted by  $-4.79$  s for C2,  $0.41$  s for C3 and  $1.30$  s for C4. (f)–(k) A zoom onto the time interval surrounding the  $B_x < 0$  excursion. (f) Same as in (b) but only the  $x$  component. (g)–(h)  $x$  and  $z$  component of the magnetic field measured by C1, C3, and C4. (i) Current density along  $y$  estimate obtained using C1, C3, and C4. (j) Estimates of the variations of  $B_x$  along  $z$  and  $B_z$  along  $x$ . Note the negative sign in front of  $\partial_x B_z$ . The data have been divided by  $\mu_0$ , the vacuum permeability, so that the sum of the two terms are the data shown in (i). (k) The two terms (black and red) contributing to the magnetic tension force along  $x$  as well as the sum of them (green). The data have been divided by  $\mu_0$  to show the force density (same unit as the  $J \times B$  force). CIS-CODIF, Cluster Ion Spectrometry - Composition and DIstribution Function analyser.

method only measuring the variations in the  $xz$  plane. A comparison between the most relevant quantities computed using three and four satellites is provided in Figure S1. The comparison shows that our calculations using three satellites are similar to those using four satellites during most of the event. This suggests that our estimates can be trusted. A clear difference can only be seen during the 05:03:50–05:04:00 UTC time interval, when the observations made by C2 significantly differ from the other three satellites. Hence, to correctly estimate the relevant quantities over the entire event, in the following we therefore use the three spacecraft method in our analysis.

In Figures 4f–k, we present a zoom onto the time interval associated with the  $B_x < 0$  excursion. We show  $V_x$  measured by C1 (Figure 4f) and data obtained from C1, C3, and C4 based of the magnetic field measurements (Figures 4g–k). The DF is observed between 05:03:20 and 05:03:40 UTC and it consists of two steps of  $B_z$  increases. The increases in  $B_z$  are also associated with clear changes in the sign of  $-\partial_x B_z$  (Figure 4j). Using the fact that earlier times in Figures 4f–k should be more earthward with respect to the DF ( $x$  increasing toward Earth), we note that  $-\partial_x B_z$  is negative (positive) when  $B_z$  is larger (smaller) earthward. At the DF ( $\sim 05:03:27$  and  $05:03:35$  UTC), we see from Figure 4 that  $B_z$  decreases earthward ( $-\partial_x B_z > 0$ ), but behind the DF,  $B_z$  increases earthward ( $-\partial_x B_z < 0$ ). These variations are responsible for the changes in the sign of  $J_y$  (Figure 4i). We also note that behind the DF (after about 05:03:35 UTC), each of the satellites measure  $B_x < 0$ . We argue that this is because of a dent in the magnetic field related to the DF. The magnetic field lines would not be entirely northward here due to the dent, but they would have a small curvature giving  $B_x < 0$  even though the spacecraft remains in the Northern Hemisphere.

The main observation of a dent is between 05:03:50 and 05:04:05 UTC. During that interval,  $B_x$  changes from positive to negative, and we suggest that this was caused by a dent in the magnetic field instead of the relative motion of the spacecraft from the Northern to the Southern Hemisphere. In this interpretation, the

satellite does not cross the symmetry plane of the magnetotail. That is, the nominal neutral sheet. Instead it moves through the dent, while remaining above the symmetry plane.

The transition from  $B_x > 0$  to  $B_x < 0$  is accompanied by a dawnward current density ( $J_y < 0$  at  $\sim 05:03:50$  UTC) which is caused by the increase of  $B_z$  earthward ( $-\partial_x B_z < 0$ ) and the decrease of  $B_x$  northward ( $\partial_z B_x < 0$ ). The decrease of  $B_x$  northward is expected when observing a magnetic dent. Indeed, in a dent,  $B_x$  decreases northward (it changes from positive to negative) and thus,  $\partial_z B_x < 0$ . We note that the use of  $J_y$  alone may not be adapted to identify a dent as  $J_y < 0$  may also be caused by the  $\partial_x B_z$  term. Hence, the term  $\partial_z B_x$  may thus be a better indicator of a magnetic dent.

To further investigate the magnetic field geometry, in Figure 4k we show the tension force along  $x$  and the individual terms comprising it. At the beginning of the interval ( $\sim 05:03:25$  UTC), the total tension force along  $x$  (green in Figure 4k) is positive, that is earthward. This is earthward of the fast flow and the DF where the magnetic field geometry is unaffected by the dent. At later times, and during a significant portion of the time when  $B_x < 0$ , we observe that the total tension force is tailward. One exception is  $\sim 05:04:03$  UTC where the force is positive while  $B_x < 0$ . This is likely due to a more complicated magnetic field geometry in all three dimensions, with significant magnetic fields also in the  $y$  direction (data not shown), and as previously shown in Movie S1, variations in the  $y$  direction can be expected for a dent.

However, the tension force being directed tailward during a significant portion of the event when  $B_x < 0$ , is a good indicator that the Cluster satellites are observing magnetic field lines with a dent geometry. We, therefore, suggest that there is a magnetic dent associated with the high-speed flow observed by the Cluster spacecraft on October 6, 2004.

## 5. Summary and Discussion

In this article, we have used a three-dimensional MHD simulation of the magnetosphere (BATS-R-US, Space Weather Modeling Framework [SWMF]) and we have investigated the effect of high-speed earthward flows in the magnetotail on the magnetic field geometry. From the simulation, we observe the existence of a dent in the magnetic field lines in the  $xz$  plane. The dent is related to the presence of a DF in the equatorial plane where the field lines are compressed and pushed toward Earth. Away from the equatorial plane, the magnetic field lines are deformed such that they wrap around the head of the high-speed flow to ultimately form a dent (Figure 1b). The dent structure is such that  $B_x > 0$  in the Southern Hemisphere and  $B_x < 0$  in the Northern Hemisphere. This is opposite to the expected signs of  $B_x$  for a standard textbook case of the magnetotail configuration earthward or the near-Earth neutral line. Such magnetic field deformations imply that it is not suitable to use the sign of  $B_x$  only to identify the hemisphere in which the observing satellite is located. Even though it is outside the scope of the present study to categorize in detail the deformation of the dawn-dusk  $B_y$  component, we also note that  $B_y$  deformations can be expected for a dent, and that this will affect how to determine in which local time sector the spacecraft is located.

From the simulation, we also see that there are three regions where currents flow near the magnetic dent (Figures 1b–d). A dawnward current is observed in the center of the dent in the middle of the plasma sheet, and the duskward currents are present above and below the dawnward current. These current signatures are different from what is the case at the middle of the plasma sheet for a more textbook-like magnetic field configuration where the cross-tail current is duskward.

In Figure 2, we have presented artificial spacecraft data for different possible crossings outside and inside the magnetic dent. Some important conclusions can be drawn when comparing data from a crossing of the cross-tail current sheet in a normal textbook geometry without a dent (Figure 2a) with crossings inside the dent. In the absence of a magnetic dent, the crossing from north to south of the center of the plasma sheet is characterized by a change of the sign of  $B_x$  from positive to negative. Also, there is a duskward component for the current density in the region where  $B_x$  changes sign ( $z = 0$ ) and the plasma beta reaches a maximum at  $z = 0$ . These properties are consistent with a spacecraft crossing the cross-tail current sheet in the center of the plasma sheet in a standard textbook magnetic field configuration.

Analysis of the artificial spacecraft data near the dent (Figures 1c and 2a–d) reveals that there are three regions where  $B_x$  vanishes. It vanishes near  $z = 1R_E$ ,  $z = 0$ , and  $z = -1R_E$ . The region near  $z = -1R_E$  has

similar properties to the  $z = 1R_E$  region, and we will thus only discuss the crossing of the  $z = 1R_E$  region. Considering a north-south crossing of the  $z = 1R_E$  region as in Figures 2a, and 2c–d, we observe that,  $B_x$  changes from positive to negative, that there is a duskward current and that the plasma beta has a local maximum. These are the properties observed near  $z = 1R_E$  but similar observations are made when a spacecraft crosses the neutral sheet in the absence of a magnetic dent. The only difference seems to be that there are additional local maxima in the plasma beta when a spacecraft crosses a dent region as compared to the case when a spacecraft crosses the plasma sheet in a normal configuration. Therefore, if a spacecraft only probes a region with duskward current, it is difficult to conclude whether the satellite really crossed the center of the plasma sheet or whether it just probed a part of a magnetic dent. However, if a satellite also measures a dawnward current together with an increase in the plasma beta, as well as signatures of a consistent  $\partial_z B_x$  and tailward tension force, it is likely that the satellite probed a magnetic dent. The region of the duskward current would be observed away from the center of the plasma sheet, while the region of dawnward current would correspond to the central part of the magnetic dent which is near the center of the plasma sheet.

In this article we have also shown data from the multi-spacecraft Cluster mission of a high-speed flow preceded by a DF. The high-speed flow was observed by all four spacecraft near  $(-15.4, 7.2, 1.8) R_E$ . The magnetic field data before the event show that the event is observed north of the neutral sheet, but we find that  $B_x$  changes from positive to negative behind the DF. Analyzing in detail the variations of the cross-tail current ( $J_y$ ), and the variations of the magnetic field component along  $x$  and  $z$  ( $\partial_x B_x$  and  $-\partial_x B_z$  which give  $J_y$ ) as well as the tension force, we suggest that the change in  $B_x$  from positive to negative is not caused by the relative motion of the satellites across the magnetotail neutral sheet from north to south. Instead the spacecraft moved through a dent caused by the high-speed flow, while continuously remaining above the neutral sheet.

In this article, we have highlighted the fact the existence of a dent in the magnetic field implies that  $B_x$  cannot be trusted alone to unambiguously determine in what hemisphere an observing spacecraft is located. For multi-spacecraft data where the spacecraft configuration is appropriate, one possible remedy is to analyze not only the  $B_x$  signatures, but also signatures in the cross-tail current and the variations in  $\partial_z B_x$  and  $-\partial_x B_z$ . However, for single-spacecraft data, there are less options for improving the determination of a spacecraft's location, but for optimal conditions, we suggest that a single-satellite method for determining the cross-tail current may be of help (Luhr et al., 1996).

Many questions naturally arise from our observations. How can one say with certainty that a magnetic dent is observed if the satellite never reaches the region of dawnward current? Are these dents always present at the front of the high-speed flows? Under which conditions can magnetic dents exist? How is the propagation of a fast flow affected by the presence of the dent, how does the dent affect the properties of the DF, and how is the injection of particles to the inner magnetosphere affected?

## Data Availability Statement

The modeling tools described in this publication are available online through the University of Michigan for download (<http://csem.engin.umich.edu/>) and are available for use at the Community Coordinated Modeling Center (CCMC; <https://ccmc.gsfc.nasa.gov/>). The Cluster data are available through the Cluster Active Science Archive, <https://csa.esac.esa.int/csa-web/>.

## References

- Angelopoulos, V., Baumjohann, W., Kennel, C. F., Coroniti, F. V., Kivelson, M. G., Pellat, R., et al. (1992). Bursty bulk flows in the inner central plasma sheet. *Journal of Geophysical Research*, 97(A4), 4027–4039. Retrieved from <https://agupubs.onlinelibrary.wiley.com/doi/abs/10.1029/91JA02701>
- Balogh, A., Carr, C. M., Acuña, M. H., Dunlop, M. W., Beek, T. J., Brown, P., et al. (2001). The cluster magnetic field investigation: Overview of in-flight performance and initial results. *Annales Geophysicae*, 19(10/12), 1207–1217. Retrieved from <https://angeo.copernicus.org/articles/19/1207/2001/>
- Baumjohann, W., Paschmann, G., & Cattell, C. (1989). Average plasma properties in the central plasma sheet. *Journal of Geophysical Research*, 94(A6), 6597–6606. Retrieved from <https://agupubs.onlinelibrary.wiley.com/doi/abs/10.1029/JA094iA06p06597>
- Birn, J. (1984). Three-dimensional computer modeling of dynamic reconnection in the magnetotail: Plasmoid signatures in the near and distant tail. In *Magnetic reconnection in space and laboratory plasmas* (pp. 264–271). American Geophysical Union (AGU). Retrieved from <https://agupubs.onlinelibrary.wiley.com/doi/abs/10.1029/GM030p0264>

## Acknowledgments

A. De Spiegeleer, M. Hamrin, H. Gunell, and T. Pitkanen. are supported by the Swedish National Space Agency grant numbers 105/14, 271/14, 108/18, and 118/17. The authors would like to thank M. Kuznetsova for the recommending the simulation. This work was carried out using the SWMF and BATS-R-US tools developed at the University of Michigan's Center for Space Environment Modeling (CSEM).

- Birn, J., Nakamura, R., Panov, E. V., & Hesse, M. (2011). Bursty bulk flows and dipolarization in MHD simulations of magnetotail reconnection. *Journal of Geophysical Research*, *116*(A1). Retrieved from <https://agupubs.onlinelibrary.wiley.com/doi/abs/10.1029/2010JA016083>
- Chen, C. X., & Wolf, R. A. (1999). Theory of thin-filament motion in earth's magnetotail and its application to bursty bulk flows. *Journal of Geophysical Research*, *104*(A7), 14613–14626. Retrieved from <https://agupubs.onlinelibrary.wiley.com/doi/abs/10.1029/1999JA900005>
- De Spiegeleer, A. (2020, January). Alexds20/bats-r-us-analysis tool. *Zenodo*. Retrieved from <https://doi.org/10.5281/zenodo.3625798>
- Escoubet, C., Schmidt, R., & Goldstein, M. (1997). *Space Science Reviews*, *79*(1/2), 11–32. Retrieved from <https://doi.org/10.1023/a:1004923124586>
- Karlsson, T., Hamrin, M., Nilsson, H., Kullen, A., & Pitkänen, T. (2015). Magnetic forces associated with bursty bulk flows in earth's magnetotail. *Geophysical Research Letters*, *42*(9), 3122–3128. Retrieved from <https://agupubs.onlinelibrary.wiley.com/doi/abs/10.1002/2015GL063999>
- Luhr, H., Warnecke, J. F., & Rother, M. K. A. (1996). An algorithm for estimating field-aligned currents from single spacecraft magnetic field measurements: A diagnostic tool applied to freja satellite data. *IEEE Transactions on Geoscience and Remote Sensing*, *34*(6), 1369–1376. <https://doi.org/10.1109/36.544560>
- Nakamura, R., Baumjohann, W., Klecker, B., Bogdanova, Y., Balogh, A., Rème, H., et al. (2002). Motion of the dipolarization front during a flow burst event observed by cluster. *Geophysical Research Letters*, *29*(20), 31–34. Retrieved from <https://agupubs.onlinelibrary.wiley.com/doi/abs/10.1029/2002GL015763>
- Nakamura, R., Baumjohann, W., Panov, E., Volwerk, M., Birn, J., Artemyev, A., et al. (2013). Flow bouncing and electron injection observed by cluster. *Journal of Geophysical Research: Space Physics*, *118*(5), 2055–2072. Retrieved from <https://agupubs.onlinelibrary.wiley.com/doi/abs/10.1002/jgra.50134>
- Ohtani, S.-i., Shay, M. A., & Mukai, T. (2004). Temporal structure of the fast convective flow in the plasma sheet: Comparison between observations and two-fluid simulations. *Journal of Geophysical Research*, *109*(A3). Retrieved from <https://agupubs.onlinelibrary.wiley.com/doi/abs/10.1029/2003JA010002>
- Panov, E. V., Nakamura, R., Baumjohann, W., Angelopoulos, V., Petrukovich, A. A., Retinò, A., et al. (2010). Multiple overshoot and rebound of a bursty bulk flow. *Geophysical Research Letters*, *37*(8). Retrieved from <https://agupubs.onlinelibrary.wiley.com/doi/abs/10.1029/2009GL041971>
- Paschmann, G., & Daly, P. W. (1998). Analysis methods for multi-spacecraft data, (Vol. 1, ISBN 1608-280X). ISSI Scientific Reports Series 1.
- Petschek, H. E., & Thorne, R. M. (1967). The existence of intermediate waves in neutral sheets. *The Astrophysical Journal*, *147*, 1157. <https://doi.org/10.1086/149105>
- Pitkänen, T., Kullen, A., Laundal, K. M., Tenfjord, P., Shi, Q. Q., Park, J. S., et al. (2019). IMF *B<sub>y</sub>* Influence on magnetospheric convection in Earth's magnetotail plasma sheet. *Geophysical Research Letters*, *46*(21), 11698–11708. <https://doi.org/10.1029/2019GL084190>
- Powell, K. G., Roe, P. L., Linde, T. J., Gombosi, T. I., & Zeeuw, D. L. D. (1999). A solution-adaptive upwind scheme for ideal magneto-hydrodynamics. *Journal of Computational Physics*, *154*(2), 284–309. Retrieved from <http://www.sciencedirect.com/science/article/pii/S002199919996299X>
- Rème, H., Aoustin, C., Bosqued, J. M., Dandouras, I., Lavraud, B., Sauvaud, J. A., et al. (2001). First multispacecraft ion measurements in and near the Earth's magnetosphere with the identical cluster ion spectrometry (CIS) experiment. *Annales Geophysicae*, *19*(10/12), 1303–1354. Retrieved from <https://angeo.copernicus.org/articles/19/1303/2001/>
- Ridley, A. J., Gombosi, T. I., & DeZeeuw, D. L. (2004). Ionospheric control of the magnetosphere: Conductance. *Annales Geophysicae*, *22*(2), 567–584. Retrieved from <https://www.ann-geophys.net/22/567/2004/>
- Sato, T., & Hayashi, T. (1979). Externally driven magnetic reconnection and a powerful magnetic energy converter. *The Physics of Fluids*, *22*(6), 1189–1202. Retrieved from <https://aip.scitation.org/doi/abs/10.1063/1.862721>
- Tóth, G., Sokolov, I. V., Gombosi, T. I., Chesney, D. R., Clauer, C. R., De Zeeuw, D. L., et al. (2005). Space weather modeling framework: A new tool for the space science community. *Journal of Geophysical Research*, *110*(A12). Retrieved from <https://agupubs.onlinelibrary.wiley.com/doi/abs/10.1029/2005JA011126>
- Tóth, G., van der Holst, B., Sokolov, I. V., Zeeuw, D. L. D., Gombosi, T. I., Fang, F., et al. (2012). Adaptive numerical algorithms in space weather modeling. *Journal of Computational Physics*, *231*(3), 870–903. Retrieved from <http://www.sciencedirect.com/science/article/pii/S002199911100088X> (Special Issue: Computational Plasma Physics).
- Vasyliunas, V. M. (1975). Theoretical models of magnetic field line merging. *Reviews of Geophysics*, *13*(1), 303–336. Retrieved from <https://agupubs.onlinelibrary.wiley.com/doi/abs/10.1029/RG013i001p00303>
- Yao, Z., Sun, W. J., Fu, S. Y., Pu, Z. Y., Liu, J., Angelopoulos, V., et al. (2013, November). Current structures associated with dipolarization fronts. *Journal of Geophysical Research: Space Physics*, *118*(11), 6980–6985. Retrieved from <https://doi.org/10.1002/2013ja019290>